International Journal of Biological Macromolecules 252 (2023) 126284

Contents lists available at ScienceDirect

International Journal of Biological Macromolecules

journal homepage: www.elsevier.com/locate/ijbiomac

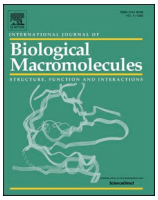

β-Cyclodextrin functionalized agarose-based hydrogels for multiple controlled drug delivery of ibuprofen

Filippo Pinelli [a], Maddalena Ponti [a], Sara Delleani [a], Fabio Pizzetti [a], Valeria Vanoli [a], Francesco Briatico Vangosa [a], Franca Castiglione [a], Havard Haugen [b], Liebert P. Nogueira [c], Arianna Rossetti [a,*], Filippo Rossi [a,*], Alessandro Sacchetti [a]

[a] Department of Chemistry, Materials and Chemical Engineering "Giulio Natta", Politecnico di Milano, Piazza Leonardo da Vinci 32, 20133 Milan, Italy
[b] Department of Biomaterials, Institute for Clinical Dentistry, University of Oslo, PO Box 1109, Blindern, NO-0317 Oslo, Norway
[c] Oral Research Laboratory, Institute for Clinical Dentistry, University of Oslo, PO Box 1109, Blindern, NO-0317 Oslo, Norway

ARTICLE INFO

Keywords:
Hydrogels
β-Cyclodextrins
Drug delivery
Controlled release

ABSTRACT

Agarose hydrogels are three-dimensional hydrophilic polymeric frameworks characterised by high water content, viscoelastic properties, and excellent ability as cell and drug delivery systems. However, their hydrophilicity as gel systems makes loading of hydrophobic drugs difficult and often ineffective. The incorporation of amphiphilic molecules (*e.g.* cyclodextrins) into hydrogels as hosts able to form inclusion complexes with hydrophobic drugs could be a possible solution. However, if not properly confined, the host compounds can get out of the network resulting in uncontrolled release. Therefore, in this work, β-cyclodextrins-based host-guest supramolecular hydrogel systems were synthesised, with β-cyclodextrins (β-CD) covalently bound to the polymeric network, preventing leakage of the host molecules. Hydrogels were prepared at two different β-CD-functionalized polyvinyl alcohol (PVA)/agarose ratios, and characterised chemically and physically. Then ibuprofen, a drug often used as a gold standard in studies involving β-CD both in its hydrophilic and hydrophobic forms, was selected to investigate the release behavior of the synthesised hydrogels and the influence of β-CD on the release. The presence of β-CD linked to the polymeric 3D network ensured a higher and prolonged release profile for the hydrophobic drug and also seemed to have some influence on the hydrophilic one.

1. Introduction

Gels fall into the soft colloids category, composed of a three-dimensional cross-linked polymeric network in which a significant amount of liquid is dispersed and retained [1,2]. Hydrogels are a peculiar subcategory of gels, in which water assumes the role of the dispersion medium [3]. The interconnections between the polymer chains and the resulting structural rigidity gives the hydrogel the capacity to not dissolve in an aqueous environment for a long period, but rather to swell and retain the molecules of water [4,5]. Those systems present a high surface area and a soft and rubbery consistency, and they are usually characterised by the presence of peculiar functional groups of polymeric chains, such as hydroxyl or carboxylic groups [6]. Hydrogels can be classified using a vast range of parameters such as the typology of cross-linking or bond, the presence of electrical surface charge or morphological features [7]. They can be used in very different fields. However, the characteristics mentioned and the drug encapsulation and release ability, along with the limitations of conventional drug administration (*i.e.*, patient compliance, high dosages, repeated administrations), ensure their extensive use in the drug delivery field [7,8]. The use of this kind of system guarantees the possibility of controlling drug release and regulating the drug's availability to cells or tissues over time. Exploiting different administration routes [9]. Hydrogels are multiscale systems, and each scale determines the properties and applications of the hydrogel in the drug delivery context [10]. The macroscopic scale affects the route by which the hydrogel is administered to the human body; on the microscopic scale, the presence or the absence of micropores influences the deformability and convective transportation of the drug; on the nanometric scale, the network formed by the polymeric cross-link is responsible for the formation of several open spaces, the size of which, called the "mesh size", plays an essential role in the drug's diffusion inside the network. Finally, at the

* Corresponding authors.
E-mail addresses: arianna.rossetti@polimi.it (A. Rossetti), filippo.rossi@polimi.it (F. Rossi).

https://doi.org/10.1016/j.ijbiomac.2023.126284
Received 26 June 2023; Received in revised form 28 July 2023; Accepted 9 August 2023
Available online 11 August 2023

molecular scale of the hydrogel, chemical interactions between the polymer and the drug are possible *via* the binding sites undoubtedly present on the polymer chains [11,12].

Of all the hydrogels, agarose-based ones show great promise in many different pathologies thanks to their high biocompatibility and the possibility of casting them in different shapes (from fibrils, to 3D printing), together with their low cost [13–15]. Moreover, their high-water content and low interfacial tension with water and biological fluids make them perfect candidates for controlled hydrophilic drug delivery [16]. However, the presence of hydrophilic groups and the characteristics of affinity with water are the reasons they are rarely used for delivering hydrophobic drugs [17]. Given that 40 % of the marketed drugs and 60 % of the therapeutic compounds being researched have a hydrophobic character, and due to the excellent features of hydrogels as drug delivery systems, the adaptation of these devices to managing the release of hydrophobic drugs is crucial, and it has drawn much attention in recent years [18,19]. One of the main strategies for extending the compatibility of hydrogels to hydrophobic APIs is the introduction into the matrix of molecules able to form inclusion complexes (*i.e.,* cyclodextrins) [20,21] or nanoparticles [22,23] that can get out of the device with an uncertain fate, if encapsulated by simple steric hindrance. Cyclodextrins (CDs) are cyclic oligosaccharides obtained by enzymatic degradation of starch [24]. They comprise six to eight glucopyranose units bound by α-1,4-glycosidic linkages. The monomers are arranged to form a truncated cone with a hydrophilic external surface (primary and secondary OH groups oriented outward) and an internal hydrophobic carbon backbone that forms a cavity (C-O-C and C—H bonds). The most commonly used CDs are α-, β- and γ-cyclodextrins, composed of six, seven and eight α-(1,4)-linked glycosyl units, respectively. Their structure is responsible for their capability to form inclusion complexes both in solution and in the solid state: a guest molecule (*i.e.*, lipophilic drug) is bound into the CD cavity, acting as a host. The formation of the inclusion complex causes important modifications to the included molecule. The most important ones are the increase in water solubility and chemical stabilisation [25]. As mentioned before, here we decided to work with β-CDs, the ones most often used in the pharmaceutical field, because their cavity size is suitable for a wide range of drugs [26–28]. In literature some systems of this kind are already presented, using different polymers [29–31].

The use of cyclodextrin to form hydrogels or to be linked to hydrogel networks has been widely studied, but a common drawback seems to be the presence of cross-linkers that limit their use due to toxic effects [32], therefore a "green route" from a chemical and biological perspective is needed [33,34]. Here we focused our attention on a simple and sustainable strategy to functionalize polymeric chains with β-CD and use them to form hydrogels without the need of cross-linkers, organic solvents or catalysts. The final aim was to build a "green" agarose-based hydrogel that could be used in multiple hydrophilic and hydrophobic drug releases. The strategy behind adding synthetic polymers to the formulation, together with agarose, can solve two main problems of agarose-based hydrogels: *i*) the absence of a reliable protocol for functionalizing their chains without using high temperatures or organic solvents, *ii*) creating a physical hydrogel with improved mechanical properties compared respect to classical agarose gels [35]. The inclusion complex formation was proved using analytical techniques, and the polymer relaxation induced by the presence of cyclodextrins induced prolonged release; on the contrary, hydrogels without cyclodextrins showed rapid drug release [36].

2. Materials and methods

2.1. Materials

The hydrogel synthesis experiments were performed using the following reagents: polyethylene glycol 2000 (PEG_{2000}, MW 2 kDa, Sigma-Aldrich Chemie GmbH, Deisenhofen, Germany), agarose (MW 200 kDa, Invitrogen Corporation, Waltham, Massachusetts), polyvinyl alcohol 15,000 (PVA_{15000}, MW 15 kDa, Sigma-Aldrich Chemie GmbH, Deisenhofen, Germany), β-cyclodextrins (MW 1135 *Da*, Sigma-Aldrich Chemie GmbH, Deisenhofen, Germany), ammonium persulfate (APS, MW 228 *Da*, Sigma-Aldrich Chemie GmbH, Deisenhofen, Germany). All other chemicals used were purchased from Sigma-Aldrich Chemie GmbH, Deisenhofen, Germany. The materials were used as received, without further purifications; solvents were of analytical grade.

2.2. Synthesis of PVA-based hydrogels

In this work, two different hydrogel formulations were investigated: one based on agarose-PVA hydrogels (AG/PVA HGs) and the same system modified with the functionalization of PVA by using β-cyclodextrins (AG/PVA-CD HGs) [37,38]. A similar procedure was used for both cases. The gels were synthesised working with an aqueous solution (2.5 mL) of agarose and PVA, and testing different mass ratios between these two macromolecules (1:1 and 1:6). Agarose/PVA 1:1 gels were prepared using 14 mg of both reagents, whereas in the case of 1:6, 14 mg of agarose and 84 mg of PVA were used. The system was irradiated using microwaves (500 W) to reach 80 °C and to initiate the gelation process. Then, during cooling and subsequent gelation, the system was subdivided into hollow metallic cylinders to obtain cylindrical gels that were easier to handle and use.

2.3. PVA functionalization with β-cyclodextrins

To synthesize the AG/PVA-CD HGs presented in the previous section, it is clear that PVA had to be chemically functionalized [39,40].

This reaction was performed by dissolving PVA (1 equivalent) in water being stirred at 60 °C and, once it was completely dissolved, APS (2 equivalents) and β-CD (10 equivalents) were added to the system. The whole solution was stirred 60 °C for 24 h. The reaction volume was then subjected to dialysis (Spectra/Por™ 3 RC 3500 Da MWCO by Thermo Fisher Scientific) against deionised water for 3 days, with daily water changes to remove the unreacted reagents. The final product was recovered by freeze-drying to obtain a white fibrous and soft solid.

2.4. NMR spectroscopy

The ^1H NMR analyses were carried out on a Brucker AC (400 MHz) spectrometer in deuterated solvents, using TMS as an internal standard. Chemical shifts (δ) in the spectra are reported in ppm, while the coupling constants J are reported in Hz. PVA functionalization was verified by comparison with reference literature and PVA spectrum. Deuterium oxide (D_2O) was used as a solvent. The ^1H HR-MAS spectra of all the hydrogel systems were recorded using a Bruker NEO 500 console (11.74 T), equipped with a dual $^1H/^{13}C$ high-resolution magic angle spinning (HR-MAS) probe for semisolid samples. Samples were transferred to a 4 mm ZrO_2 rotor containing a volume of about 12 μL. All the ^1H HR-MAS spectra were acquired at 298 K with 8 scans, a relaxation delay of 5 s and a spinning rate of 4 kHz.

2.5. Hydrogel characterization: SEM and nano-CT

The hydrogel samples obtained were lyophilised and characterised using scanning electron microscopy (SEM) and nano-computed tomography (nano-CT). SEM analyses were done using a Zeiss Evo50 with EDS Bruker Quantax 200 to reproduce the inner framework of those systems in two-dimensions. The nano-CT investigation was done in a nano-computed tomography (nano-CT) device (SkyScan 2211 Multiscale X-ray Nano_CY System, Bruker micro-CT, Kontich, Belgium) using a 20–190 kV tungsten X-ray source and a dual detection system: an 11-megapixel cooled 4032 × 2670 pixel CCD-camera and a 3-megapixel 1920 × 1536 pixel CMOS flat panel.

The samples were scanned at 38 kV, 370 μA and 1400 ms. The scans

were taken over 180° with a rotation step of 0.14° and a voxel size of 800 nm using the CCD detector. Projections were reconstructed using the system-provided software, NRecon (version 1.7.4.6), and analyzed using CTAn (Bruker micro-CT, version 1.18.4.0).

2.6. Rheology analysis: amplitude sweep tests

The rheological properties of the materials were investigated by running amplitude sweep tests to determine the sample's linear viscoelastic region, the storage modulus (G′) and the loss modulus (G″). This analysis was carried out using an Anton Paar MCR 502 rheometer with a Parallel Plates measuring system (diameter 25 mm, plate-plate distance 0.5 mm). The shear strain amplitude range was between 0.01 % and 100 %. Angular frequency was 10 rad/s; tests were carried out at 25 °C.

2.7. Swelling tests

Swelling tests were carried out at room temperature on lyophilised hydrogels to investigate their ability to swell and retain water [41]. Duplicate tests were done for each gel formulation, in order to favour proof of reliability. Freeze dried hydrogels were first weighed to determine the dry mass of each of them and then incubated in a closed vial with a sufficient volume of distilled water to cover the whole gel mass. At precise time intervals, gels were extracted from the vials, freed from excess water and weighed. For each scheduled time of weighting, the swelling ratio was determined using the following Eq. (1):

$$Q\ [\%] = \frac{wet\ mass\ (t) - dry\ mass}{dry\ mass} \bullet 100 \tag{1}$$

The results are presented as the systems' swelling ratio as a function of time.

2.8. Drug loading and release tests

To test the release from the hydrogels, the gels were loaded with a gold standard drug bearing both a hydrophilic and a hydrophobic nature: sodium ibuprofen (IBU-Na) and ibuprofen (IBU). First, both drugs were dissolved separately in a PBS solution and left stirring at room temperature for 1 week with PVA-CD, in order to promote the inclusion inside the host molecules, until equilibrium between their solubility and loading was reached. The flasks were covered and the stirring occurred in the dark to prevent any photodegradation of the compounds. Then, for the same purpose of preventing any degradation, during the HG formulation, loading of the PVA-CD-IBU (or PVA-CD-IBU-Na) into the HG matrix was carried out after an MW irradiation process on the agarose, during cooling at 45 °C and prior to gelation, using the PBS PVA-CD-IBU (or PVA-CD-IBU-Na) solutions prepared previously. The loading solution was added directly to the system during gelation at a 2:1 ratio between the volume of the gel and the drug solution (the quantities of reactants were therefore in proportion to the total volume of the solution). The final formulation was subdivided into hollow metallic cylinders to obtain cylindrical gels (diameter 1 cm) and after 30 min of storing at 4 °C the loaded gels were formed, and kept to rest at 4 °C overnight to complete gelation. The release tests were then performed placing each sample in a 24-well PCR plate, covered by 2 mL of PBS solution (0.1 M, pH 7.4). The multi-well was stored statically in a stove at 37 °C to simulate the human biological temperature; at regular intervals of time one millilitre of the solvent enriched by the drug released was sampled and substituted by a fresh millilitre of PBS to avoid varying the test volume and restore the concentration gradient in order to promote drug release. Each sample was then analyzed by means of UV–vis spectroscopy; the analyses were performed in triplicate on different samples and the absorbance data obtained was then averaged. The concentration of IBU (or IBU-Na) in each sample was determined, after subtracting the absorbance of PVA-CD, by applying the Lambert-Beer equation, that makes it possible to quantify the concentration of substances by measuring their absorption of UV–vis radiation.

2.9. Mathematical modelling in order to estimate drug diffusivity

The drug diffusivities (D) of IBU-Na and IBU were evaluated using a mathematical model based on mass balances, *i.e.*, fundamental conservation laws [42]. Diffusion is described by the second Fick law with a 1-dimensional model in a cylindrical geometry, as presented in Eq. (2). Here, radius (r) is the characteristic dimension for the transportation phenomenon investigated. Therefore, an increase in mean drug concentration is triggered by the material flux, which takes place at the PBS/hydrogel surface. Eqs. (6) and (7) represent the boundary conditions for the left and the right border, respectively. The former implies profile symmetry at the centre (in relation to the cylindrical axis), while the latter represents the equivalence between the material's diffusive fluxes at the PBS/hydrogel surface. The entire set of equations for the model then reads as follows:

$$\frac{\partial C_G}{\partial t} = D\frac{1}{r^2}\frac{\partial}{\partial r}\left(r^2\frac{\partial C_G}{\partial r}\right) \tag{2}$$

$$V_S\frac{\partial C_G}{\partial t} = k_C S_{exc}(C_G - C_S) \tag{3}$$

$$C_S(t=0) = 0 \tag{4}$$

$$C_G(t=0) = C_{G,0} = \frac{m_{G,0}}{V_G} \tag{5}$$

$$\left.\frac{\partial C_G}{\partial r}\right|_{r=0} = 0 \tag{6}$$

$$-D\left.\frac{\partial C_G}{\partial r}\right|_{r=R} = k_C(C_G - C_S) \tag{7}$$

The two mass balance equations (Eqs. (2) and (3) with Eqs. (4) and (5) as initial conditions) involve the mean drug concentration within the hydrogel (C_G), the mean drug concentration in the outer solution (C_S), the volume of the solution (V_S), the hydrogel volume (V_G), the drug mass inside the matrix (m_G) and the interfacial exchange surface (S_{exc}), *i.e.* the boundary surface between gel and surrounding solution (which can be considered here to be the side surface only, as a simplification). Finally, D represents the diffusion coefficient and k_C the mass transfer coefficient. The latter is computed using the Sherwood number (Sh) obtained by means of a penetration theory expressed according to Eq. (8):

$$Sh = \frac{8}{\pi} = \frac{k_C \bullet 2r}{D} \tag{8}$$

The solution of Eqs. (2)–(3) was calculated numerically, assuming that the gel dimensions remain constant, the latter being a reasonably valid assumption as degradation phenomena occur much slower than delivery.

2.10. Statistical analysis

Experimental data were analyzed using One-way ANOVA test was used and then followed by Bonferroni's post-hoc test. The statistical significance was set to a p value <0.05. The results are presented as the mean ± standard deviation value. The measurements are reported as mean ± standard deviation, calculated on the three different samples involved in the experimental analyses.

3. Results and discussion

3.1. Hydrogel synthesis and characterization

The incorporation of β-CD into hydrogel networks started with the formation of covalent bonds between PVA chains and β-CD. The reaction

took place at 60 °C in water, adding only APS as the initiator (Fig. 1a). The reaction mechanism is described in the Supporting Information section (Fig. S2). The advantages of this reaction are due to the low temperature used, the absence of toxic solvents and the use of a biocompatible initiator, that makes it ideal in terms of sustainability. The efficacy of this route is confirmed by NMR analyses (Fig. S1a–f), in which characteristic peaks of PVA (around 4 ppm) and β-CD (5.13 ppm) are clearly visible. On the basis of the integrations reported in Fig. S1e, it is possible to estimate the grafting degree: by identifying the peak at 5.13 ppm as that for the hydrogen that belongs to the anomeric C of the cyclodextrin, it is possible to compare its integral with that of the -CH- peak of PVA at 4.09 ppm. The integration reveals that there is a grafting of 1 CD for each 46 -CH- units over a total of 341, which gives an estimation of a 13 % degree of grafting on the polymer. This degree of functionalization was tuned in order to preserve hydroxyl groups that can interact with agarose chains (Fig. 1b). Hydrogel formation occurs by means of physical interactions between PVA-CD and agarose chains during microwave-assisted gelation. The onset of gelation onset was achieved by means of electromagnetic stimulation (500 W irradiated power) heating at a rate of 1 min per 10 mL of polymeric solution at 80 °C. Microwave-enhanced chemistry is based on efficient heating of materials by "microwave dielectric heating" effects that can occur without catalysts. As gelation proceeds, the system viscosity increases continuously, decreasing the probability of interaction between polymeric chains. This physico-chemical condition results in a "welding" between microgel surfaces, giving rise to the final three-dimensional macrostructure. During the hydrogel cooling phase, slightly above 37 °C, the agarose solution can be mixed with PVA-CD-drug solutions: this procedure guarantees that good mixing still occurs during the sol state, *i.e.* before sol/gel transition, without any possible API degradation.

The three-dimensional network obtained is a physical hydrogel with H bonds between hydroxyl groups of PVA and agarose, responsible for the formation of the 3D structure. The FTIR spectrum of AG/PVA hydrogel (Fig. 1c) shows the characteristic bands of agarose such as the C–O–C and glycosidic linkage at 1065 cm^{-1}. The absorption bands at 931 and 893 cm^{-1} are associated with 3,6-anhydrogalactose and the C—H bending vibrations of anomeric carbon in ß-galactose residues, respectively. Slight changes in the intensity and peak position are observed respect to agarose alone (Fig. S3). For instance, the two peaks of AG at 1062 and 1044 cm^{-1} shift to higher frequencies at 1065 and 1047 cm^{-1}; these changes underline the formation of inter-molecular

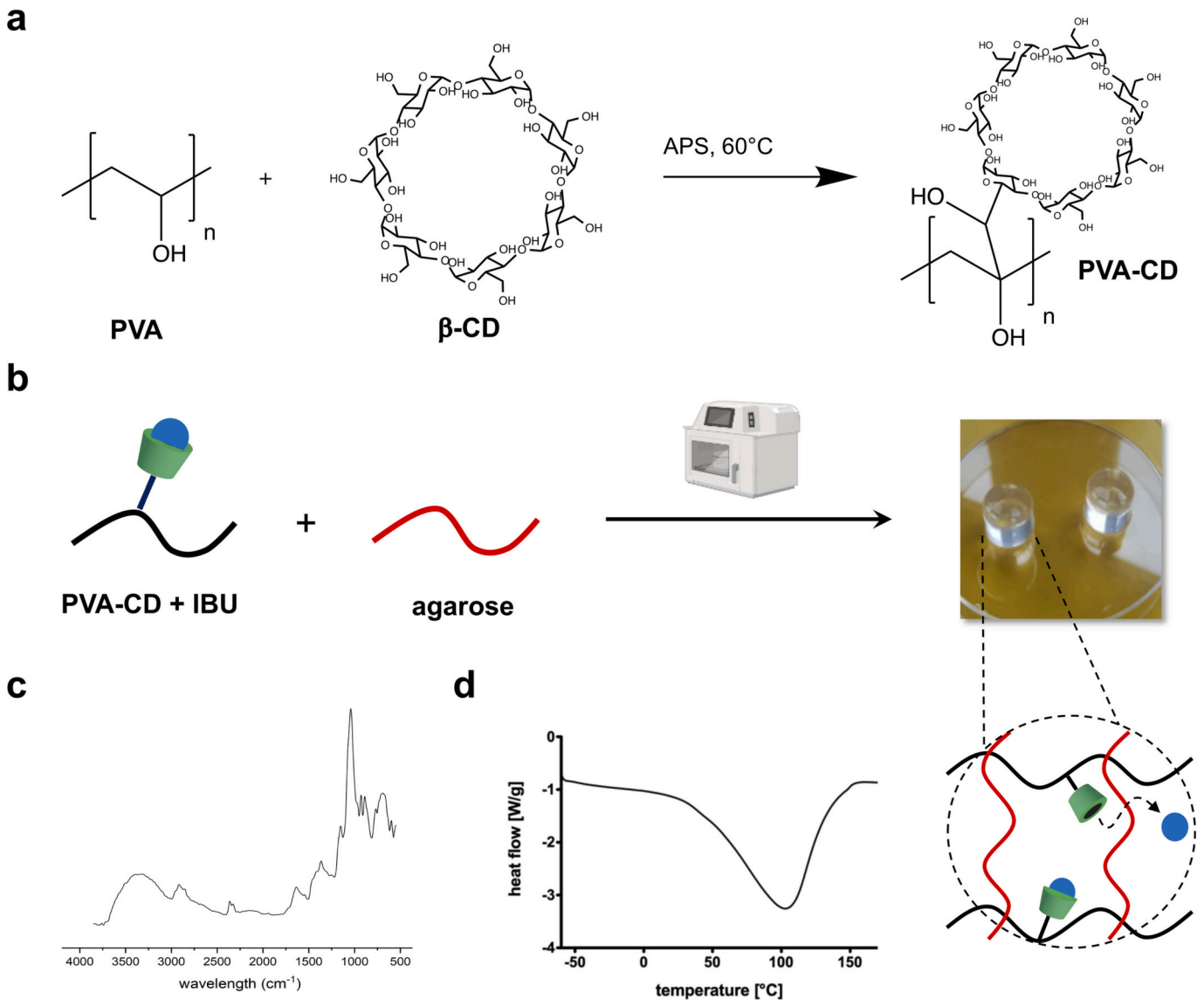

Fig. 1. a) Reaction scheme for PVA-CD; b) schematic representation of microwave-assisted gelation of agarose and PVA-CD loaded with IBU; c) FTIR spectrum of AG/PVA-CD hydrogel; d) DSC thermogram of AG/PVA-CD hydrogel.

hydrogen bonds between AG and PVA as observed in other studies [43,44]. The gel obtained showed a glass transition temperature of 45 °C, a value that is between that of agarose and PVA gels [45,46].

Of the various hydrogel formulations tested, we selected the ones with an agarose/PVA mass ratio of 1:1 (from now on called "AG/PVA1:1") and of 1:6 (from now on called "AG/PVA1:6") to compare the behavior of gels with a significantly different amount of polymer and β-cyclodextrins within their structures (AG/PVA-CD1:1 and AG/PVA-CD1:6). HR-MAS NMR spectroscopy was then used to characterise the gels obtained and verify the presence of the β-CD within the system's final structure. The strongest peaks in the ^{1}H HR MAS spectrum (Fig. 2a) are only due to free monomers or free short polymeric chains that are not linked to the gel's network. In the HGs spectrum, the characteristic signals of -CH_2- and -CH- are visible at 3.97 ppm and 1.64 ppm, respectively, which characterise the system [47]. At the same time, in the HGs spectrum, the peaks that belong to the β-CD moiety are visible in the region 3.5–4 ppm and anomeric resonance is observed at 5.0 ppm [48]. Small upfield chemical shift variations are observed for protons H6, H5, H3 and H1 of β-CD when comparing the ^{1}H spectrum of β-CD dissolved in an aqueous solution and the HGs system (see SI Fig. S9). Based on this, the low-intensity peaks give evidence of the binding of the PVA and the cyclodextrins in the hydrogels' matrices. These peculiar peaks are not present in the spectrum of the formulation without the β-CD moiety, and for this reason their presence in the hydrogel with the functionalized PVA is unambiguous. In Fig. 2a we show the ^{1}H HR-MAS spectrum for AG/PVA-CD1:1 that is equal to that for AG/PVA-CD1:6. Additional spectra and comparisons between the different gels with pure PVA and the functionalized one, for AG/PVA1:1 are given in the Supporting Information section. The materials were then characterised using SEM analysis to achieve detailed information about the samples' surface and internal morphology. The SEM images of the samples are shown in Fig. 2b for AG/PVA-CD1:1 and AG/PVA-CD1:6 hydrogels. Both the formulations present high porosity and, consequently high surface area with a homogenous aspect. It is worth observing, although, that in the case of the AG/PVA-CD1:6 formulation, the smaller mesh size for AG/PVA-CD1:1 (in the range of 30 μm) produces a denser network; furthermore, the edges of each pore are better defined.

It is noticeable, as a consequence, that there is an increased number of crosslinking points due to the higher polymer concentration. Thickening of the network when passing from AG/PVA-CD1:1 to AG/PVA-CD1:6 may be responsible for the different Q values found in the swelling tests, as presented in the next section. Indeed, in general, the higher the cross-linking density, the lower the swelling abilities. Similar conclusions can be obtained by observing the AG/PVA HGs present in the Supporting Information section.

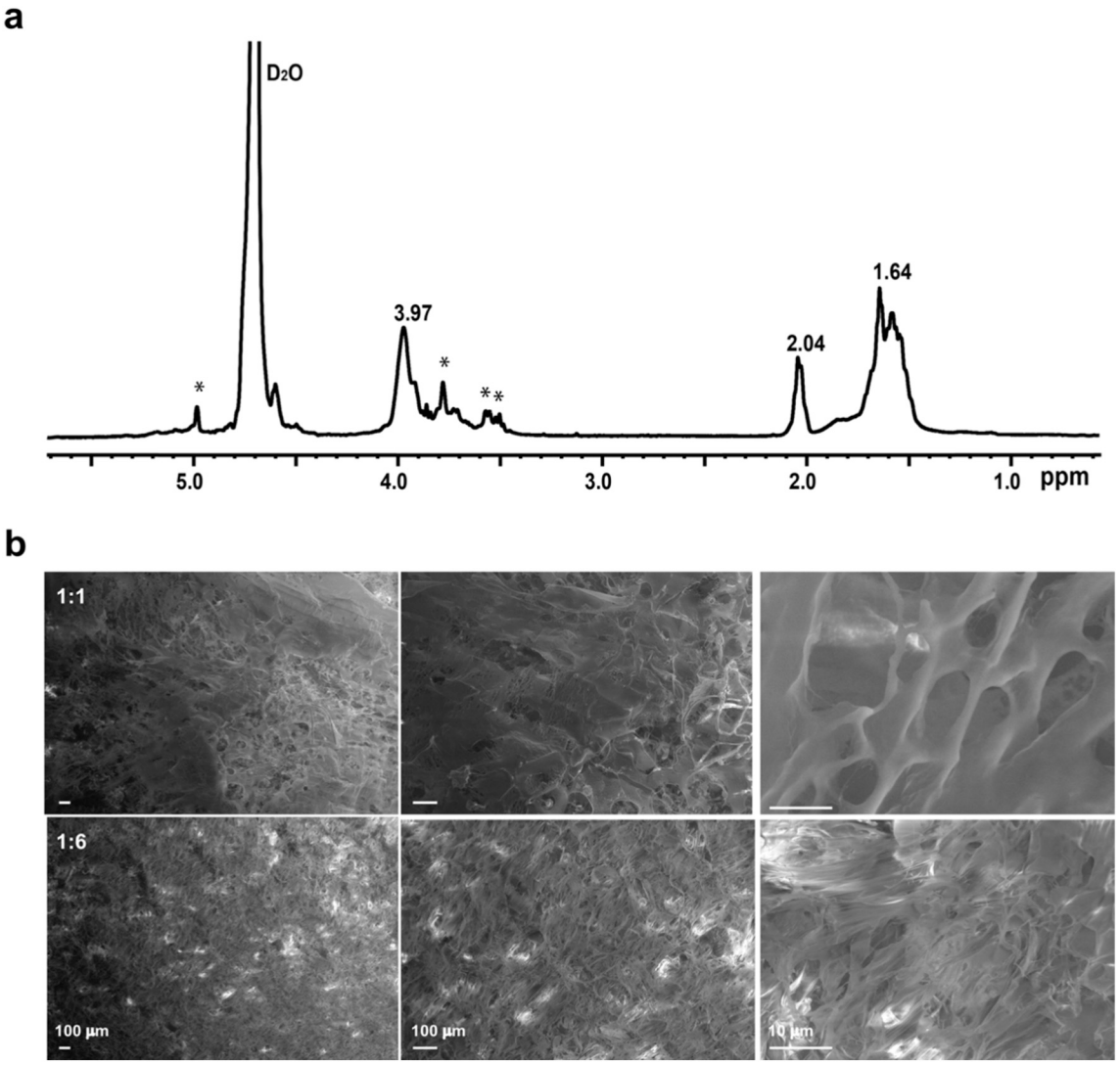

Fig. 2. a) ^{1}H HR-MAS spectrum of the AG/PVA-CD HGs (* indicate the β-CD resonances); b) SEM images of the AG/PVA-CD1:1 hydrogels and AG/PVA-CD1:6 hydrogels. Scale bars = 100 μm and 10 μm.

3.2. Nano-CT analysis

As already mentioned, for the formulations both with and without the β-CD, the samples' morphology consists of large polymeric sheets and the structure appears to be homogeneous. We continued investigation of the inner structure of the gel networks using a nano-CT, high-resolution cross-sectional imaging technique that uses X-rays to create cross-sections of the sample, building a virtual system model, with the advantage of not destroying the original one. We applied this technique to compare the inner structures for both HGs that were functionalized and those without *β*-CD to observe the effect of the presence of different quantities of the polymers and the influence of *β*-CD. In Figs. 3 and 4, the nano-CT analyses of the AG/PVA1:1 formulation without and with *β*-CD and AG/PVA1:6 without and with *β*-CD are shown.

From the analysis, in AG/PVA1:1 HGs the dimensions of the pores were estimated to be in the range of 100 μm, with a total porosity (almost full open porosity) of 98.4 % and a connectivity density of 7×10^{-6} μm $^{-3}$. In the case of AG/PVA-CD1:6 HGs the dimensions of the pores were smaller, in the range of 40 μm, the total porosity (still full open porosity) of 97 % and a connectivity density of 3×10^{-5} μm $^{-3}$.

From the results obtained, we can observe that the formulation with a higher amount of PVA presents higher connectivity and smaller pore dimensions confirming an influence in this formulation study. These differences can be observed in both the 3D rendering presented in the figure and in the 2D map drawn using nano-computed tomography. As to the role of *β*-CD, as seen in the SEM analysis, its presence does not change the macro properties of the hydrogels for both the 1:1 and 1:6 formulations.

3.3. Swelling tests

The swelling tests, conducted on the lyophilized hydrogels as discussed in the previous section, showed a swift swelling process in all the cases analyzed, which corresponds to quick expansion of the hydrogels' network englobing the aqueous incubation solution. This process stands until the osmotic pressure reaches the same value in the hydrogel's bulk and in the external environment (swelling equilibrium). This equilibrium point is identified in the swelling plots by achieving a plateau, as can be seen in Fig. 5a and b.

As can be seen from the plots, similar trends are reported in the formulation with and without *β*-cyclodextrins in both cases. This confirms that the greatest influence on the HGs' ability to swell is related to the polymeric composition of the matrix and not to the presence of *β*-CD functionalization. This result is in accordance with literature studies where agarose increases the swelling ability of the hydrogels respect to neat PVA [49,50]. Comparing the two formulations AG/PVA1:1 and AG/PVA1:6 great differences are visible in the maximum swelling of the framework and following Nano-CT images. The explanation of this critical difference must be sought in the increasing quantity of PVA in the AG/PVA1:6 formulation. This is responsible for increased cross-linking density in the gel framework, making its swelling mechanism more difficult.

3.4. Rheological characterization

Fig. 6 shows dynamic strain sweep tests (DSS) performed at 37 °C for AG/PVA-CD1:1 and AG/PVA-CD1:6 gel samples. For both formulations the storage modulus (G′) was found to be approximately one order of magnitude higher than the loss modulus (G″), indicating a solid-like rather than liquid-like material.

It is clearly visible that hydrogel's behavior is dominated at low strain values by the elastic component of the modulus. With the increase in strain values, the structure of the network breaks down and the elastic modulus decreases steeply. The crossover strain can be readily identified as the value after which the contribution of G″ becomes predominant compared to G′, and is higher for AG/PVA1:1 than for AG/PVA1:6. This is in accordance with the fact that the G′ and G″ curves for AG/PVA1:6 are shifted on slightly minor values compared to AG/PVA1:1. This can be associated with the higher amount of PVA in the formulation. Moreover, we observed for both the AG/PVA1:1 formulation and for the AG/PVA1:6 one that the presence of the β-CD does not affect the rheological properties of the hydrogels and the same crossover strain was found in the same formulation of AG/PVA HGs and AG/PVA-CD HGs (details in Supporting Information). Moreover the addition of PVA increased the rheological properties of agarose gels compared to a study in literature, in that the G′ and G″ are around 1000 and 100 Pa, compared to the study in literature in which G′ and G″ are around 200 and 10 Pa, respectively [35,51].

3.5. Drug release assays

The drug release ability of AG/PVA HGs was tested considering the behavior of these systems with ibuprofen, a commonly commercialised and gold standard drug with well-known affinity for the *β*-CD cavity [52–54]. We conducted drug release tests with both ibuprofen sodium salt (IBU-Na), with a hydrophilic nature and not able to enter the *β*-CD, and classical ibuprofen (IBU), which is a hydrophobic molecule in its acidic form, that can interact with *β*-CD as a guest as observed in previous study [55]. In the figure below (Fig. 7) the release trends of the IBU-Na are reported for the two different formulations with and without

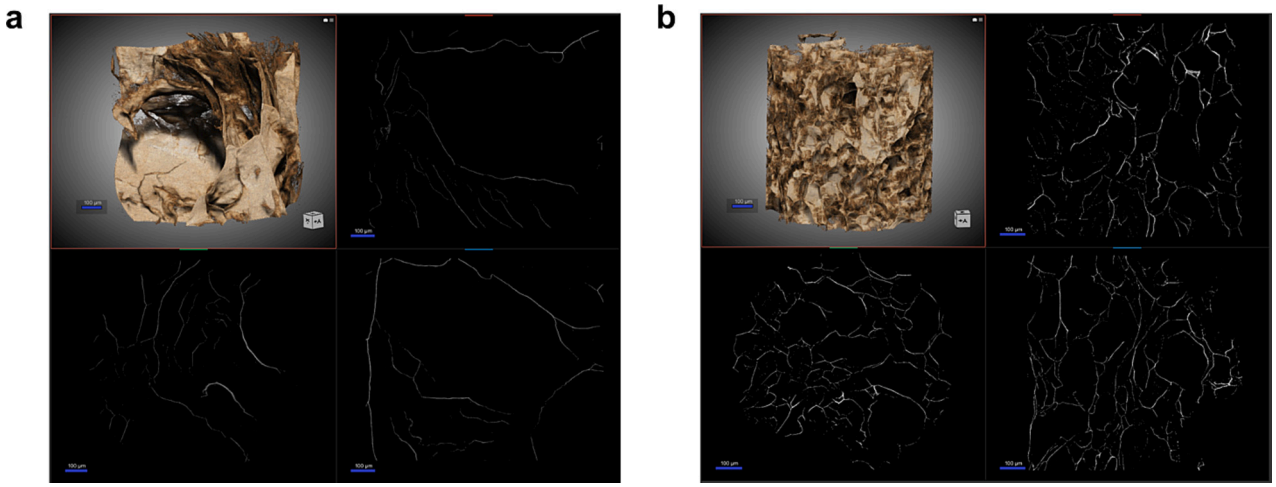

Fig. 3. Nano-CT images of the formulation AG/PVA1:1 a) without *β*-CD and with; b) with *β*-CD. Scale bars: 100 μm.

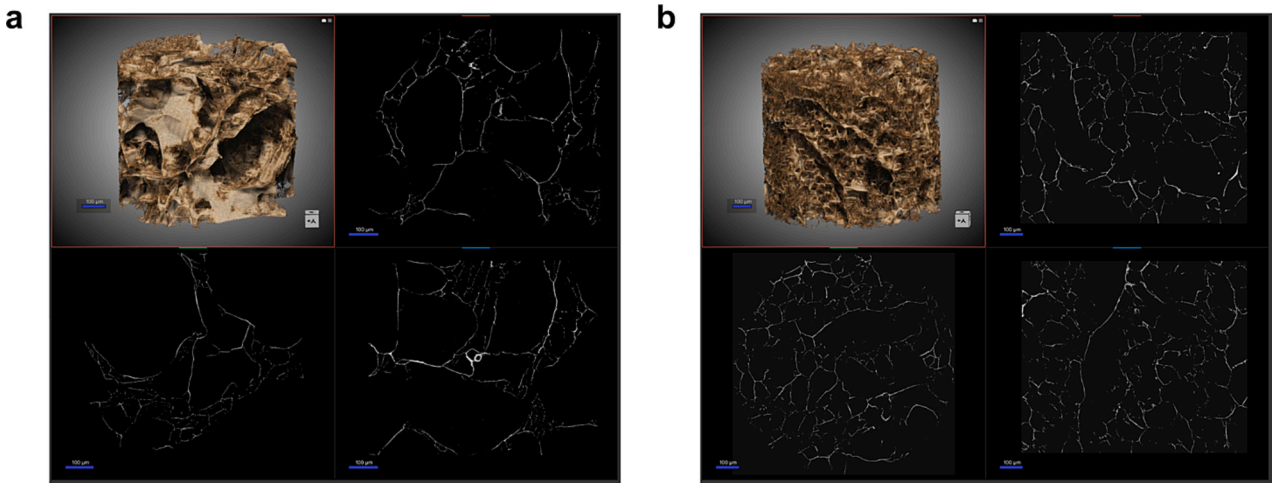

Fig. 4. Nano-CT images of the AG/PVA1:16 formulation a) without β-CD and with b) with β-CD. Scale bars: 100 μm.

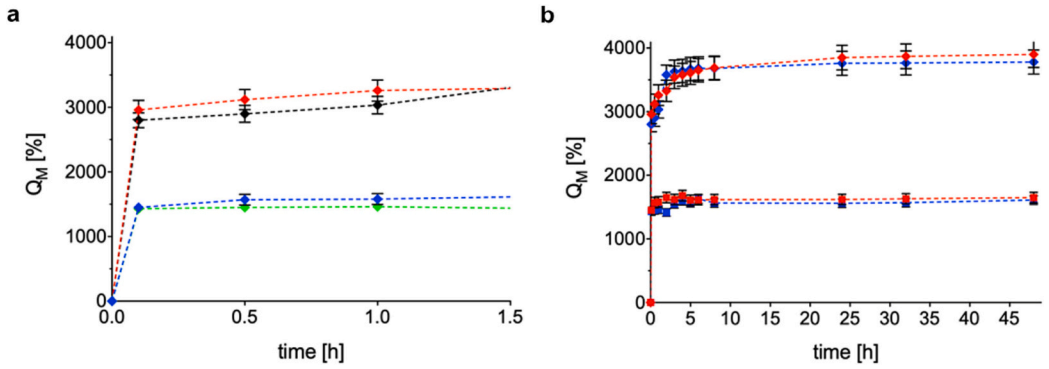

Fig. 5. Swelling trend of AG/PVA1:1 (blue rhombuses), AG/PVA-CD1:1 (red rhombuses), AG/PVA1:6 (blue squares), AG/PVA-CD1:6 (red squares). a) zoom in the initial hours; b) general swelling trend. (For interpretation of the references to colour in this figure legend, the reader is referred to the web version of this article.)

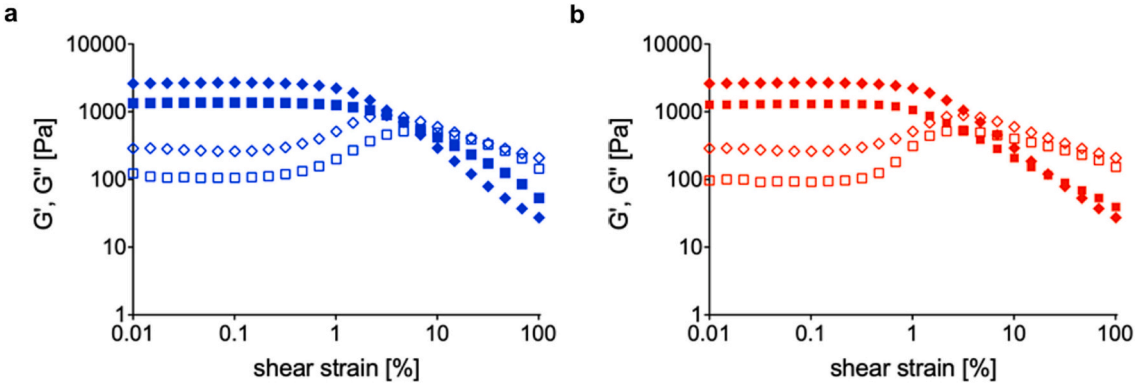

Fig. 6. Comparison between the amplitude sweep test conducted on: a) AG/PVA1:1 hydrogels (blue rhombuses, G′ ◆ and G″ ⋄) and AG/PVA1:6 hydrogels (blue squares, G′ ■, G″ □); b) AG/PVA-CD1:1 hydrogels (red rhombuses, G′ ◆ and G″ ⋄) and AG/PVA-CD1:6 hydrogels (red squares, G′ ■, G″ □). (For interpretation of the references to colour in this figure legend, the reader is referred to the web version of this article.)

β-CD. Considering the 1:1 formulations, AG/PVA-CD1:1 HGs presented higher release in the initial hours and a larger total release is reported compared to other samples. On the other hand, in the case of the 1:6 formulation, no difference can be detected in the initial hours of release, whereas at longer times a slightly higher release can be observed for AG/PVA-CD1:6 HGs. These differences demonstrated that the presence of β-CD can also modulate the release of IBU-Na, promoting a quicker release in presence of functionalization. This can be explained by considering a direct influence of the cyclodextrins on the sodium ibuprofen: even if it cannot be encapsulated inside the cavity of β-CD, its solubility and subsequent release can be influenced by the presence of cyclodextrin reducing its coordination with water [56]. This is evident if we compare its release with the release of rhodamine B, a hydrophilic drug mimetic that does not interact with β-CD and it is similar to IBU-Na in terms of hydrodynamic diameter [57,58]. From Fig. S8 it is evident how rhodamine B delivery kinetics are only influenced by the ratios of the polymers within the formulation and not by the presence/absence of cyclodextrin. For IBU-Na it is also possible to observe that the 1:6

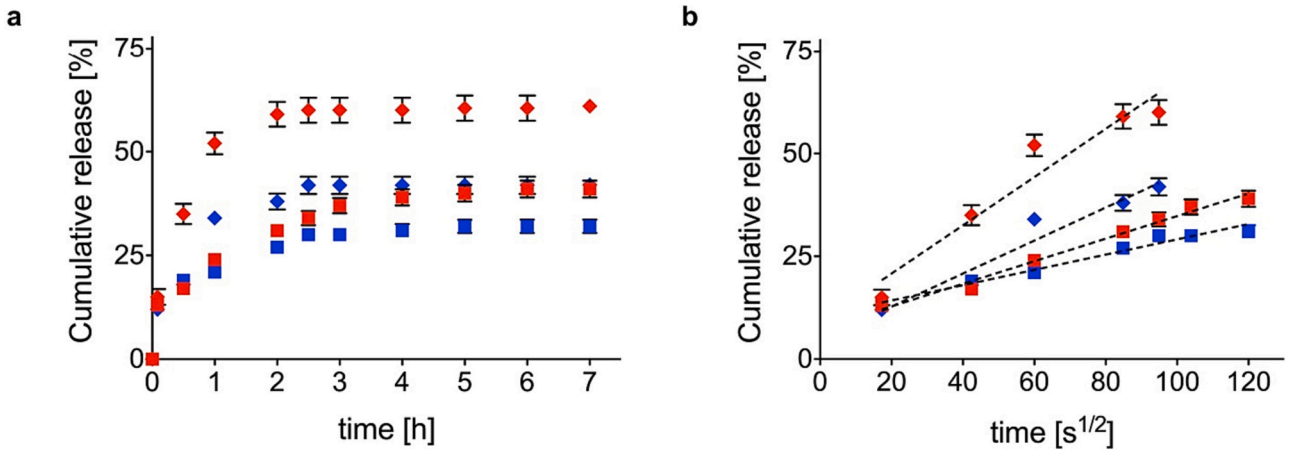

Fig. 7. a) Cumulative release trend of IBU-Na from AG/PVA1:1 HGs (blue rhombuses), AG/PVA-CD1:1 HGs (red rhombuses), AG/PVA1:6 HGs (blue squares), AG/PVA-CD1:6 HGs (red squares); b) comparison between the slopes of IBU-Na release from HGs against the square root time. This is representative of the Fickian diffusion coefficient of IBU-Na in gels ($p < 0.0001$ between all of the groups). The values are calculated as a percentage of the total mass loaded (mean value ± standard deviation is plotted). (For interpretation of the references to colour in this figure legend, the reader is referred to the web version of this article.)

formulation (Fig. 7b) presented a longer linear trend, representative of Fickian diffusion, and a more sustained release driven by stronger interactions within the 1:6 network. Burst release, that describes the uncontrolled instantaneous loss of a loaded drug, is around 15 % for both IBU-Na and rhodamine B and does not depend on either cross-linking density and or the presence of β-CD. These values underline the good release performance of AG/PVA HGs, which are very low considering the high hydrophilicity of IBU-Na and rhodamine B [59].

At the same time, we also tested the release of ibuprofen in its acidic form (IBU) from the hydrogel matrix, in order to verify if the HGs' release ability for this hydrophobic drug could be improved by applying the β-cyclodextrins (Fig. 8). Its release profile can be explained by considering the presence of a host-guest interaction with the β-cyclodextrins. Indeed, their presence promotes the solubility of ibuprofen in the system and the subsequent availability for the release, despite its hydrophobic nature [23]. IBU release occurs without any burst release, as reported in Fig. 8. For comparison, the value of IBU burst release in the case of AG/PVA HGs without β-CD is around 20 %. As to the role of different polymer ratios in the formulations we can observe that here, unlike the previous case, this is a factor that does not influence the release rates for AG/PVA HGs.

Mass release data obtained experimentally was used to estimate diffusion coefficients of drug molecules released from AG/PVA and AG/PVA-CD hydrogels. As explained above, the release mechanism could be considered as a pure Fickian diffusion, allowing us to neglect any contribution of both swelling and degradation phenomena. Table 1 shows the dependence of diffusivity on hydrogel formulation and the presence or not of β-CD within the network. In accordance with release studies in literature, the diffusion coefficients obtained have a magnitude of the order of 10^{-9} m^2/s [60]. The diffusivity values for sodium ibuprofen are similar to previous studies conducted on agarose gels [61], with the influence given by the presence of cyclodextrins. Indeed, as said, the presence of β-CD can change the water coordination of IBU-Na molecules making the motion through the polymer 3D network quicker. In addition, a strong influence is also given by the formulation used that influences the 3D network in terms of mean mesh size and intermolecular forces.

Table 1
Diffusion coefficients of drugs within AG/PVA 1:1, AG/PVA-CD1:1, AG/PVA1:6 and AG/PVA-CD1:6 hydrogels. * $p < 0.5$ against AG/PVA 1:1 IBU-Na, ** $p < 0.01$ against AG/PVA 1:1 IBU-Na, $^{\#}$ $p < 0.5$ against AG/PVA 1:1 IBU, $^{\#\#}$ $p < 0.01$ against AG/PVA 1:1 IBU.

	Diffusivity[a] [m^2/ s]			
drug	AG/PVA1:1	AG/PVA-CD1:1	AG/PVA1:6	AG/PVA-CD1:6
IBU-Na	1.22 ± 0.10	1.42 ± 0.12$^{\#}$	0.84 ± 0.03$^{*,\#}$	1.02 ± 0.07$^{*,\#}$
IBU	1.13 ± 0.08	0.08 ± 0.13$^{**,\#\#}$	0.92 ± 0.09*	0.07 ± 0.01$^{**,\#\#}$

[a] All values have to be multiplied by 10^{-9}.

4. Conclusions

Designing hydrogels able to release not only hydrophilic but also hydrophobic drugs is a pivotal point for their medical application. In this study, we used a simple and sustainable strategy to functionalize polymeric chains with β-cyclodextrins and then form agarose-based hydrogels to address this issue. The key advantages of the approach are the

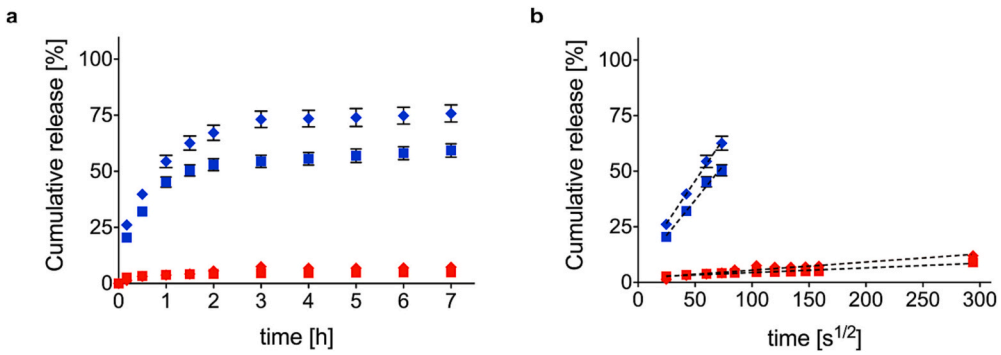

Fig. 8. a) Cumulative release trend of IBU from AG/PVA1:1 HGs (blue rhombuses), AG/PVA-CD1:1 HGs (red rhombuses), AG/PVA1:6 HGs (blue squares), AG/PVA-CD1:6 HGs (red squares); b) comparison between the slopes of IBU release from HGs against the square root time. This is representative of the Fickian diffusion coefficient of IBU in gels ($p < 0.0001$ between all of the groups). The values are calculated as a percentage of the total mass loaded (mean value ± standard deviation is plotted). (For interpretation of the references to colour in this figure legend, the reader is referred to the web version of this article.)

absence of cross-linkers, organic solvents or catalysts. The formulations synthesised showed a storage modulus approximately one order of magnitude higher than the loss modulus, indicating an elastic rather than viscous material with higher properties than the classical physical agarose-based hydrogel formulations. The "green" agarose-based hydrogel synthesised was then tested as an efficient multiple-drug release system of hydrophilic and hydrophobic drugs. Sodium ibuprofen was used as a hydrophilic drug; despite it not being able to create a proper inclusion complex with β-CD, its release is partially influenced by the presence of β-CD in the networks and mostly by the formulation used (ratio between AG and PVA). On the other hand, ibuprofen is a highly hydrophobic drug, and its release is greatly influenced by the formation of host-guest complexes with β-CD, more than the formulation used. All these findings represent a first step that can be useful for developing and tuning specific agarose-based hydrogels as tools for multiple drug delivery.

CRediT authorship contribution statement

Filippo Pinelli: Methodology, Validation, Writing – original draft. **Maddalena Ponti:** Methodology. **Sara Delleani:** Methodology. **Fabio Pizzetti:** Methodology. **Valeria Vanoli:** Methodology. **Francesco Briatico Vangosa:** Methodology, Validation. **Franca Castiglione:** Methodology, Validation. **Havard Haugen:** Methodology, Validation. **Liebert P. Nogueira:** Methodology. **Arianna Rossetti:** Methodology, Validation, Supervision, Writing – review & editing. **Filippo Rossi:** Conceptualization, Supervision, Writing – review & editing. **Alessandro Sacchetti:** Conceptualization, Supervision, Writing – review & editing.

Declaration of competing interest

The authors declare that they have no known competing financial interests or personal relationships that could have appeared to influence the work reported in this paper.

Data availability

Data will be made available on request.

Appendix A. Supplementary data

Supplementary data to this article can be found online at https://doi.org/10.1016/j.ijbiomac.2023.126284.

References

[1] J. Li, D.J. Mooney, Designing hydrogels for controlled drug delivery, Nat. Rev. Mater. 1 (2016) 16071.
[2] F. Pinelli, O.F. Ortola, P. Makvandi, G. Perale, F. Rossi, In vivo drug delivery applications of nanogels: a review, Nanomedicine 15 (2020) 2707–2727.
[3] M. Mahinroosta, Z. Jomeh Farsangi, A. Allahverdi, Z. Shakoori, Hydrogels as intelligent materials: a brief review of synthesis, properties and applications, Mater. Today Chem 8 (2018) 42–55.
[4] C.A. Dreiss, Hydrogel design strategies for drug delivery, Curr. Opin. Colloid Interface Sci. 48 (2020) 1–17.
[5] F. Pinelli, L. Magagnin, F. Rossi, Progress in hydrogels for sensing applications: a review, Mater. Today Chem. 17 (2020), 100317.
[6] Q. Ma, Q. Li, X. Cai, P. Zhou, Z. Wu, B. Wang, W. Ma, S. Fu, Injectable hydrogels as drug delivery platform for in-situ treatment of malignant tumor, J. Drug Deliv. Sci. Technol. 76 (2022), 103817.
[7] B. Sharma, R. Bharti, R. Sharma, Controlled drug delivery: "a review on the applications of smart hydrogel", Mater. Today Proc. 65 (2022) 3657–3664.
[8] J. Zheng, X. Song, Z. Yang, C. Yin, W. Luo, C. Yin, Y. Ni, Y. Wang, Y. Zhang, Self-assembly hydrogels of therapeutic agents for local drug delivery, J. Control. Release 350 (2022) 898–921.
[9] M. Rizwan, R. Yahya, A. Hassan, M. Yar, A.D. Azzahari, V. Selvanathan, F. Sonsudin, C.N. Abouloula, pH sensitive hydrogels in drug delivery: brief history, properties, swelling, and release mechanism, material selection and applications, Polymers 9 (2017) 137.
[10] P. Kesharwani, A. Bisht, A. Alexander, V. Dave, S. Sharma, Biomedical applications of hydrogels in drug delivery system: an update, J. Drug Deliv. Sci. Technol. 66 (2021), 102914.
[11] M.J. Penn, M.G. Hennessy, Optimal loading of hydrogel-based drug-delivery systems, Appl. Math. Model. 112 (2022) 649–668.
[12] M. Moghadam, M.S. Seyed Dorraji, F. Dodangeh, H.R. Ashjari, S.N. Mousavi, M. H. Rasoulifard, Design of a new light curable starch-based hydrogel drug delivery system to improve the release rate of quercetin as a poorly water-soluble drug Eur, J. Pharm. Sci. 174 (2022), 106191.
[13] I. Caron, F. Rossi, S. Papa, R. Aloe, M. Sculco, E. Mauri, A. Sacchetti, E. Erba, N. Panini, V. Parazzi, M. Barilani, G. Forloni, G. Perale, L. Lazzari, P. Veglianese, A new three dimensional biomimetic hydrogel to deliver factors secreted by human mesenchymal stem cells in spinal cord injury, Biomaterials 75 (2016) 135–147.
[14] M. Gao, P. Lu, B. Bednark, D. Lynam, J.M. Conner, J. Sakamoto, M.H. Tuszynski, Templated agarose scaffolds for the support of motor axon regeneration into sites of complete spinal cord transection, Biomaterials 34 (2013) 1529–1536.
[15] C. Yang, Q. Ren, X. Liu, Y. Liu, B. Zhang, P. Zhou, H. Li, Porous agarose/Gd-hydroxyapatite composite bone fillers with promoted osteogenesis and antibacterial activity, Ceram. Int. 48 (2022) 9413–9425.
[16] M.J. Afshari, M. Sabzi, L. Jiang, Y. Behshad, A.R. Zanjanijam, G.R. Mahdavinia, M. Ahmadi, Incorporation of dynamic boronate links and Ag nanoparticles into PVA hydrogels for pH-regulated and prolonged release of methotrexate, J. Drug Deliv. Sci. Technol. 63 (2021), 102502.
[17] Y. Xiao, Y. Gu, L. Qin, L. Chen, X. Chen, W. Cui, F. Li, N. Xiang, X. He, Injectable thermosensitive hydrogel-based drug delivery system for local cancer therapy, Colloids Surf. B Biointerfaces 200 (2021), 111581.
[18] L. Zhao, G. Shen, G. Ma, X. Yan, Engineering and delivery of nanocolloids of hydrophobic drugs, Adv. Colloid Interf. Sci. 249 (2017) 308–320.
[19] D. Gu, A.J. O'Connor, G.G.H. Qiao, K. Ladewig, Hydrogels with smart systems for delivery of hydrophobic drugs, Expert Opin. Drug Deliv. 14 (2017) 879–895.
[20] B. Ari, S. Demirci, R.S. Ayyala, B. Salih, N. Sahiner, Superporous poly (β-Cyclodextrin) cryogels as promising materials for simultaneous delivery of both hydrophilic and hydrophobic drugs, Eur. Polym. J. 176 (2022), 111399.
[21] C. Langer, R. Süss, HPLC-DAD-CAD-based approach for the simultaneous analysis of hydrophobic drugs and lipid compounds in liposomes and for cyclodextrin/drug inclusion complexes, J. Pharm. Biomed. Anal. 201 (2021), 114120.
[22] F. Rossi, R. Ferrari, F. Castiglione, A. Mele, G. Perale, D. Moscatelli, Polymer hydrogel functionalized with biodegradable nanoparticles as composite system for controlled drug delivery, Nanotechnology 26 (2015), 015602.
[23] A. Mellati, E. Hasanzadeh, M. Gholipourmalekabadi, S.E. Enderami, Injectable nanocomposite hydrogels as an emerging platform for biomedical applications: a review, Mater. Sci. Eng. C 131 (2021), 112489.
[24] M.E. Davis, M.E. Brewster, Cyclodextrin-based pharmaceutics: past, present and future, Nat. Rev. Drug Discov. 3 (2004) 1023–1035.
[25] L.X. Song, L. Bai, X.M. Xu, J. He, S.Z. Pan, Inclusion complexation, encapsulation interaction and inclusion number in cyclodextrin chemistry, Coord. Chem. Rev. 253 (2009) 1276–1284.
[26] V. Aiassa, C. Garnero, M.R. Longhi, A. Zoppi, Cyclodextrin multicomponent complexes: pharmaceutical applications, Pharmaceutics 13 (2021) 1099.
[27] R. Lakkakula, R.W. Maçedo Krause, A vision for cyclodextrin nanoparticles in drug delivery systems and pharmaceutical applications, Nanomedicine 9 (2014) 877–894.
[28] P. Jansook, N. Ogawa, T. Loftsson, Cyclodextrins: structure, physicochemical properties and pharmaceutical applications, Int. J. Pharm. 535 (2018) 272–284.
[29] C. Qian, P. Yan, G. Wan, S. Liang, Y. Dong, J. Wang, Facile synthetic Photoluminescent graphene quantum dots encapsulated β-cyclodextrin drug carrier system for the management of macular degeneration: detailed analytical and biological investigations, J. Photochem. Photobiol. B Biol. 189 (2018) 244–249.
[30] C.H. Nguyen, K.S. Banh, C.H. Dang, C.H. Nguyen, T.D. Nguyen, β-Cyclodextrin/alginate nanoparticles encapsulated 5-fluorouracil as an effective and safe anticancer drug delivery system, Arab. J. Chem. 15 (2022), 103814.
[31] M.E. Di Pietro, M. Ferro, A. Mele, Drug encapsulation and chiral recognition in deep eutectic solvents/β-cyclodextrin mixtures, J. Mol. Liq. 311 (2020), 113279.
[32] G.S. Krishnakumar, S. Sampath, S. Muthusamy, M.A. John, Importance of crosslinking strategies in designing smart biomaterials for bone tissue engineering: a systematic review, Mater. Sci. Eng. C 96 941–954.
[33] J. Gao, J.M. Karp, R. Langer, N. Joshi, The future of drug delivery, Chem. Mater. 35 (2023) 359–363.
[34] E. Larraneta, S. Stewart, M. Ervine, R. Al-Kasasbeh, R.F. Donnelly, Hydrogels for hydrophobic drug delivery. classification, synthesis and applications, J. Funct. Biomater. 9 (2018) 13.
[35] M. Ghebremedhin, S. Seiffert, T.A. Vilgis, Physics of agarose fluid gels: rheological properties and microstructure, Curr. Res. Food Sci. 4 (2021) 436–448.
[36] S.S. Braga, Cyclodextrin superstructures for drug delivery, J. Drug Deliv. Sci. Technol. 75 (2022), 103650.
[37] C. Kim, D. Jeong, S. Kim, Y. Kim, S. Jung, Cyclodextrin functionalized agarose gel with low gelling temperature for controlled drug delivery systems, Carbohydr. Polym. 222 (2019), 115011.
[38] J. Shao, Z. Zhang, S. Zhao, S. Wang, Z. Guo, H. Xie, Self-healing hydrogel of poly (vinyl alcohol)/ agarose with robust mechanical property, Starch 71 (2019) 1800281.
[39] Q. Lu, N. Li, J. Li, Supramolecular adsorption of cyclodextrin/polyvinyl alcohol film for purification of organic wastewater, J. Polym. Eng. 40 (2020) 158–172.
[40] R.M. Sarfraz, M. Ahmad, A. Mahmood, M.R. Akram, A. Abrar, Development of β-cyclodextrin-based hydrogel microparticles for solubility enhancement of rosuvastatin: an in vitro and in vivo evaluation, Drug Des. Devel. Ther. 11 (2017) 3083–3096.

[41] J. Liao, B. Hou, H. Huang, Preparation, properties and drug controlled release of chitin-based hydrogels: an updated review, Carbohydr. Polym. 283 (2022), 119177.
[42] F. Rossi, R. Ferrari, S. Papa, D. Moscatelli, T. Casalini, G. Forloni, G. Perale, P. Veglianese, Tunable hydrogel—nanoparticles release system for sustained combination therapies in the spinal cord, Colloids Surf. B 108 (2013) 169–177.
[43] M. Sabzi, N. Samadi, F. Abbasi, G.R. Mahdavinia, M. Babaahmadi, Bioinspired fully physically cross-linked double network hydrogels with a robust, tough and self-healing structure, Mater. Sci. Eng. C 74 (2017) 374–381.
[44] E. Al-Emam, H. Soenen, J. Caen, K. Janssens, Characterization of polyvinyl alcohol-borax/agarose (PVA-B/AG) double network hydrogel utilized for the cleaning of works of art, Herit. Sci. 8 (2020) 106.
[45] T. Remiš, P. Bělský, T. Kovářík, J. Kadlec, M. Ghafouri Azar, R. Medlín, V. Vavruňková, K. Deshmukh, K.K. Sadasivuni, Study on structure, thermal behavior, and viscoelastic properties of nanodiamond-reinforced poly (vinyl alcohol) nanocomposites, Polymers 13 (2021) 1426.
[46] R. Medina-Esquivel, Y. Freile-Pelegrin, P. Quintana-Owen, J.M. Yanez-Limon, J. J. Alvarado-Gil, Measurement of the sol–gel transition temperature in agar, Int. J. Thermophys. 29 (2008) 2036–2045.
[47] Q. Zhang, M. Zhang, T. Wang, X. Chen, Q. Li, X. Zhao, Preparation of aloe polysaccharide/honey/PVA composite hydrogel: antibacterial activity and promoting wound healing, Int. J. Biol. Macromol. 211 (2022) 249–258.
[48] X. Fan, J. Geng, Y. Wang, H. Gu, PVA/gelatin/β-CD-based rapid self-healing supramolecular dual-network conductive hydrogel as bidirectional strain sensor, Polymer 246 (2022), 124769.
[49] J. Shao, Z. Zhang, S. Zhao, S. Wang, Z. Guo, H. Xie, Y. Hu, Self-healing hydrogel of poly (vinyl alcohol)/agarose with robust mechanical property, Starch 71 (2019) 1800281.
[50] H. Li, C. Wu, S. Wang, W. Zhang, Mechanically strong poly (vinyl alcohol) hydrogel with macropores and high porosity, Mater. Lett. 266 (2020), 127504.
[51] B. Kopka, B. Kost, J. Wrzesniewska, K. Rajkowska, S. Kadlubowski, A. Kunicka-Styczynska, A. Baryga, W. Gonciarz, M. Basko, M. Brzezinski, Supramolecular poly (vinyl alcohol)-based hydrogels containing quercetin for bacterial and fungal elimination, Eur. Polym. J. 187 (2023), 111881.
[52] S. Pereva, V. Nikolova, T. Sarafska, S. Angelova, T. Spassov, T. Dudev, Inclusion complexes of ibuprofen and β-cyclodextrin: supramolecular structure and stability, J. Mol. Struct. 1205 (2020), 127575.
[53] M. Erdős, M. Frangou, T.J.H. Vlugt, O.A. Moultos, Diffusivity of α-, β-, γ-cyclodextrin and the inclusion complex of β-cyclodextrin: ibuprofen in aqueous solutions; A molecular dynamics simulation study, Fluid Phase Equilib. 528 (2021), 112842.
[54] J. Wang, F. Yang, Preparation of 2-hydroxypropyl-β-cyclodextrin polymers crosslinked by poly(acrylic acid) for efficient removal of ibuprofen, Mater. Lett. 284 (2021), 128882.
[55] P.M. Dewland, S. Reader, P. Berry, Bioavailability of ibuprofen following oral administration of standard ibuprofen, sodium ibuprofen or ibuprofen acid incorporating poloxamer in healthy volunteers, BMC Clin. Pharmacol. 9 (2009) 19.
[56] S.D. Deosarkar, R.T. Sawale, A.D. Arsule, A.L. Puyad, Volumetric and ultraacoustic properties of sodium salts of ibuprofen/ diclofenac drugs in aqueous and aqueous-β-cyclodextrin solution, J. Mol. Liq. 297 (2020), 111812.
[57] G. Gonzalez, A. Sagarzazu, T. Zoltan, Infuence of microstructure in drug release behavior of silica nanocapsules, J. Drug Deliv. 1 (2013), 803585.
[58] A.J. Bain, P. Chandna, J. Bryant, Picosecond polarized fluorescence studies of anisotropic fluid media. I. Theory, J. Chem. Phys. 112 (2000) 10418–10434.
[59] J. Yoo, Y.Y. Won, Phenomenology of the initial burst release of drugs from PLGA microparticles, ACS Biomater. Sci. Eng. 6 (2020) 6053–6062.
[60] E. Axpe, D. Chan, G.S. Offeddu, Y. Chang, D. Merida, H.L. Hernandez, E.A. Appel, A multiscale model for solute diffusion in hydrogels, Macromolecules 52 (2019) 6889–6897.
[61] F. Rossi, F. Castiglione, M. Salvalaglio, M. Ferro, M. Moioli, E. Mauri, M. Masi, A. Mele, On the parallelism between the mechanisms behind chromatography and drug delivery: the role of interactions with a stationary phase, Phys. Chem. Chem. Phys. 19 (2017) 11518.